

FIG. 1. Experimental measurement of friction for transitional flows with slugs. These flows consist of laminar plugs and slugs. To make slugs, we perturb the flow using an iris. (a) Data points (f, Re) corresponding to laminar flows (shown in black), transitional flows (shown in blue), and turbulent flows (shown in red). The dashed line is the friction for laminar flow, $f_{\text{lam}}(Re)$; the solid line is the friction for turbulent flow, $f_{\text{turb}}(Re)$ (the Blasius law). (b) The time series $f(t)$ and the attendant probability distribution function $p(f)$ for the data points marked L, S, and T in panel (a). Note that for the transitional data point S, $f(t)$ swings between two distinct values, f_- and f_+ , where $f_- = f_{\text{lam}}(Re)$ and $f_+ = f_{\text{turb}}(Re)$, as indicated in panel (a). Here, f_- is the friction for laminar plugs, confirming that laminar plugs are indeed laminar, and f_+ is the friction for slugs, suggesting that slugs are turbulent. This conclusion holds for all the transitional data points of panel (a).

data points that fall on $f_{\text{turb}}(Re)$ and correspond to turbulent flows; and data points that fall between $f_{\text{lam}}(Re)$ and $f_{\text{turb}}(Re)$ and correspond to transitional flows. Here, all transitional flows are transitional flows with slugs. In Fig. 1b, we show the time series $f(t)$ and the attendant probability distribution function $p(f)$ for a representative laminar data point (marked L), for a representative transitional data point (marked S), and for a representative turbulent data point (marked T). For point L and for point T, $p(f)$ has a single peak, the value of which is the same as the long-time average of $f(t)$, which we have denoted by f . By contrast, for the transitional data point S, $p(f)$ has two peaks and $f(t)$ swings [12] between the peak values, marked f_- and f_+ in Fig. 1, spending little time at the long-time average of $f(t)$, which includes contributions from both laminar plugs and slugs. Here, f_- is the friction for laminar plugs (that is, the unitless pressure drop per unit length of laminar plug) and f_+ is the friction for slugs (that is, the unitless pressure drop per unit length of slug). But there is more: it turns out that $f_- = f_{\text{lam}}(Re)$ and $f_+ = f_{\text{turb}}(Re)$ (as indicated in Fig. 1a)—and not just for data point S but for all transitional data points in Fig. 1a. This finding confirms that laminar plugs are indeed laminar, and, more important, it suggests that slugs are turbulent.

We now turn to transitional flows with puffs. Unlike slugs, puffs are short ($\approx 20 D$ long) as compared to the lengthspan $\Delta L = 202 D$, and the technique we have used

to measure f for slugs cannot be used for puffs. To measure f for puffs, we create a train of puffs [13, 14] such that at any given time about 6-7 puffs fit within ΔL . We then measure the time series $f(t)$, which we average over a long time to obtain f . Now, this f includes contributions from both puffs and laminar plugs. To disentangle these contributions, we use the procedure described in Methods (SM); this procedure yields f for puffs and f for laminar plugs. Note that the same procedure can be applied to transitional flows with slugs, as an alternative to the simpler procedure that we used to obtain the results of Fig. 1b (the results differ by $< 1.5\%$).

In Fig. 2a, a log-log plot of f vs. Re , we show all of the transitional data points that we have measured. For each of the transitional data points that we have measured in Fig. 2a, we compute f for flashes (either slugs or puffs, as the case might be) and f for laminar plugs, and plot the results in Fig. 2b. For all transitional flows, f for laminar plugs equals $f_{\text{lam}}(Re)$ and f for flashes equals $f_{\text{turb}}(Re)$, irrespective of the type of flash. Thus, by the conventions of fluid dynamics going back to the times of Reynolds, flash flow is turbulent flow.

To adduce further experimental evidence that flash flow is indeed turbulent flow, we turn to Kolmogorov's phenomenological theory of turbulence [15, 16], a theory that provides a thorough, empirically-tested description of the statistical structure of turbulent flow. Central to the phenomenological theory is the turbulent-energy spectrum $E(k)$, which represents the way in which the

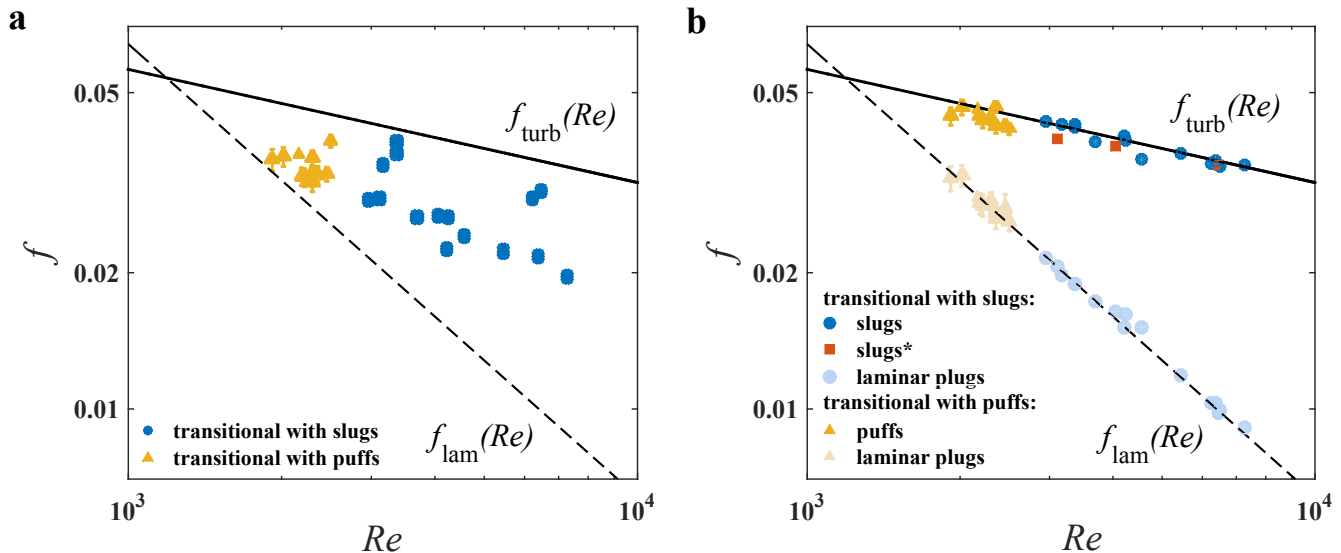


FIG. 2. Experimental measurement of friction for transitional flows. (a) Data points (f, Re) corresponding to transitional flows with slugs (shown in blue) and transitional flows with puffs (shown in yellow). For each data point, f includes a contribution from laminar plugs and a contribution from flashes (either slugs or puffs, as the case might be). By disentangling these contributions we obtain f for laminar plugs (f_-) and f for flashes (f_+). In panel (b) we show the data point (f_-, Re) and the data point (f_+, Re) for each and every data point in panel (a). In all cases, f_- falls on $f_{\text{lam}}(Re)$, confirming that laminar plugs are indeed laminar, and f_+ falls on $f_{\text{turb}}(Re)$, indicating that flashes, irrespective of type, are turbulent. All data points (panels a and b) have error bars. The vertical error bars indicate errors in f (see Supplementary Text in SM); they are mostly smaller than the size of the data points. The errors in Re are in all cases smaller than the size of the data points. In panel (b), for the data points marked with *, we compute f for slugs using the same procedure that we use to compute f for puffs.

turbulent kinetic energy is distributed among turbulent fluctuations of different wavenumbers k in a flow. Kolmogorov argued that, for $Re \rightarrow \infty$ and for k in the “universal range” $k \gg D^{-1}$, $E(k)$ depends only on k , ν , and $\varepsilon \propto U^3/D$, irrespective of the flow, where ε is the turbulent power (that is, the rate at which turbulent kinetic energy is dissipated in the flow). In this case, Kolmogorov predicted that [15, 16]

$$E(k) \propto \frac{\nu^2}{\eta} F(k\eta), \quad (1)$$

which is known as small-scale universality, and

$$\eta \propto DRe^{-3/4}, \quad (2)$$

where F is a universal function and η is the viscous lengthscale. Further, for k in the “inertial range” $D^{-1} \ll k \ll \eta^{-1}$, a subset of the universal range, $E(k) \propto \varepsilon^{2/3} k^{-5/3}$, which is known as the “5/3 law.” Eq. (1), Eq. (2), and the 5/3 law are asymptotic results associated with the limit $Re \rightarrow \infty$, and it is not possible to predict mathematically for what finite value of Re they might be expected to hold within a preset tolerance. In practice, it is only feasible to verify the 5/3 law over a broad inertial range, which necessitates a small ratio η/D , which in turn necessitates a particularly large value of Re (due to the small exponent of Re in Eq. (2)). Indeed, in pipe

flows the 5/3 law becomes clearly apparent [17] only for $Re > 80,000$, well above the values of Re at which flashes have been observed. By contrast, Eq. (1) and Eq. (2) can hold in principle at the values of Re of our experiments (also see [18, 19]). Note, however, that whereas the 5/3 law can be tested by carrying out a single experiment at a very high value of Re , a test of Eq. (1) and Eq. (2) requires that many experiments be carried out over a broad range of values of Re .

To compute $E(k)$ we start by measuring a time series of the axial velocity at the centerline of the pipe, $u(t)$, using laser Doppler velocimetry (LDV). In Fig. 3a we plot $u(t)$ for three representative flows: a turbulent flow, a transitional flow with slugs, and a transitional flow with puffs; for the transitional flows, the segments of $u(t)$ corresponding to flashes have been shaded in grey. Using time series such as those of Fig. 3a, we compute $E(k)$ and η for several turbulent flows, slug flows, and puff flows (see Methods in SM). In Fig. 3b, we show a few representative spectra $E(k)$, along with a few high- Re spectra from the Princeton superpipe experiment [17, 20]. The spectra of Fig. 3b have been rescaled in order to verify small-scale universality (Eq. (1)). At high $k\eta$, the rescaled spectra $\eta E(k)/\nu^2$ vs. $k\eta$ converge onto the universal function $F(k\eta)$ of Eq. (1) for turbulent flows as well as for flash flows, in keeping with small-scale universality. Further, the rescaled spectra peel off from $F(k\eta)$ at

a value of $k\eta$ that lessens monotonically as Re increases, irrespective of the type of flow.

In Fig. 3c, we test Eq. (2) using data points from all our experiments along with a few high- Re data points from the Princeton superpipe experiment [20]. Irrespective of the type of flow, the data points, which span about two decades in Re , are in keeping with Eq. (2). From Figs. 3b and 3c, we conclude that the spectra and the viscous lengthscales of flash flows, like those of conventional turbulent flows, are governed by the phenomenological theory of turbulence, with the implication that flash flows, aside from their being restricted to relatively low Re , are statistically indistinguishable from conventional turbulent flows.

In a number of experimental and computational studies [21–23] published in 2016, compelling evidence has been adduced in support of a 30 year-old conjecture by Yves Pomeau [24] to the effect that the subcritical transition in pipe flow and other shear flows belongs to the directed-percolation universality class of non-equilibrium phase transitions. Yet, in a comment on those studies, titled “The Long and Winding Road,” Pomeau [25] cautioned that “the arrowhead patterns observed in early experiments [on boundary layers] are sufficiently regular to denote a bifurcation to a turbulence-free state.” That is to say, if flashes were non-turbulent, they could hardly be the agents of a transition to turbulence, and the experimental and computational evidence of directed percolation would be severed from the turbulent regime. Our findings indicate that, at least for pipe flow, flashes display fluid-frictional behavior diagnostic of turbulence and a statistical structure indistinguishable from that of conventional turbulent flow in the sense of Kolmogorov. Thus, we conclude that flash flow is but turbulent flow, and flashes endow the transitional regime with the requisite link to turbulence. Our findings suggest that new insights into the transition to turbulence may be gained by approaching the transition from above, from higher to lower Re , complementing the usual approach from below. The long road keeps winding.

We thank Prof. Jun Sakakibara (Meiji University) and Mr. Makino (Ni-gata company) for help with the experimental setup. This work was supported by the Okinawa

Institute of Science and Technology Graduate University.

-
- [1] O. Reynolds, P. Roy. Soc. Lond. **35**, 84 (1883).
 - [2] I. Wygnanski and F. Champagne, J. Fluid Mech. **59**, 281 (1973).
 - [3] I. Wygnanski, M. Sokolov, and D. Friedman, J. Fluid Mech. **69**, 283 (1975).
 - [4] B. Eckhardt, T. M. Schneider, B. Hof, and J. Westerweel, Annu. Rev. Fluid Mech. **39**, 447 (2007).
 - [5] T. Mullin, Annu. Rev. Fluid Mech. **43**, 1 (2011).
 - [6] D. Barkley, J. Fluid Mech. **803**, P1 (2016).
 - [7] K. Avila, D. Moxey, A. de Lozar, M. Avila, D. Barkley, and B. Hof, Science **333**, 192 (2011).
 - [8] D. Barkley, B. Song, V. Mukund, G. Lemoult, M. Avila, and B. Hof, Nature **526**, 550 (2015).
 - [9] H. Schlichting, “Boundary-layer theory,” (McGraw-Hill, 1979) Chap. 20.
 - [10] G. Gioia and F. Bombardelli, Phys. Rev. Lett. **88**, 014501 (2002).
 - [11] G. Gioia and P. Chakraborty, Phys. Rev. Lett. **96**, 044502 (2006).
 - [12] F. Durst and B. Ünsal, J. Fluid Mech. **560**, 449 (2006).
 - [13] D. Samanta, A. De Lozar, and B. Hof, J. Fluid Mech. **681**, 193 (2011).
 - [14] B. Hof, A. De Lozar, M. Avila, X. Tu, and T. M. Schneider, Science **327**, 1491 (2010).
 - [15] A. N. Kolmogorov, Dokl. Akad. Nauk. SSSR **30**, 299 (1941), [English translation in Proc. Roy. Soc. Lond. Ser. A 434 (1991)].
 - [16] U. Frisch, *Turbulence: The Legacy of A.N. Kolmogorov* (Cambridge University Press, 1995).
 - [17] B. Rosenberg, M. Hultmark, M. Vallikivi, S. Bailey, and A. Smits, J. Fluid Mech. **731**, 46 (2013).
 - [18] J. Schumacher, K. R. Sreenivasan, and V. Yakhot, New J. Phys. **9**, 89 (2007).
 - [19] J. Schumacher, J. D. Scheel, D. Krasnov, D. A. Donzis, V. Yakhot, and K. R. Sreenivasan, P. Nat. Acad. Sci. USA **111**, 10961 (2014).
 - [20] S. C. Bailey, M. Hultmark, J. Schumacher, V. Yakhot, and A. J. Smits, Phys. Rev. Lett. **103**, 014502 (2009).
 - [21] M. Sano and K. Tamai, Nature Phys. **12**, 249 (2016).
 - [22] G. Lemoult, L. Shi, K. Avila, S. V. Jalikop, M. Avila, and B. Hof, Nature Phys. **12**, 254 (2016).
 - [23] H.-Y. Shih, T.-L. Hsieh, and N. Goldenfeld, Nature Phys. **12**, 245 (2016).
 - [24] Y. Pomeau, Phys. D **23**, 3 (1986).
 - [25] Y. Pomeau, Nature Phys. **12**, 198 (2016).

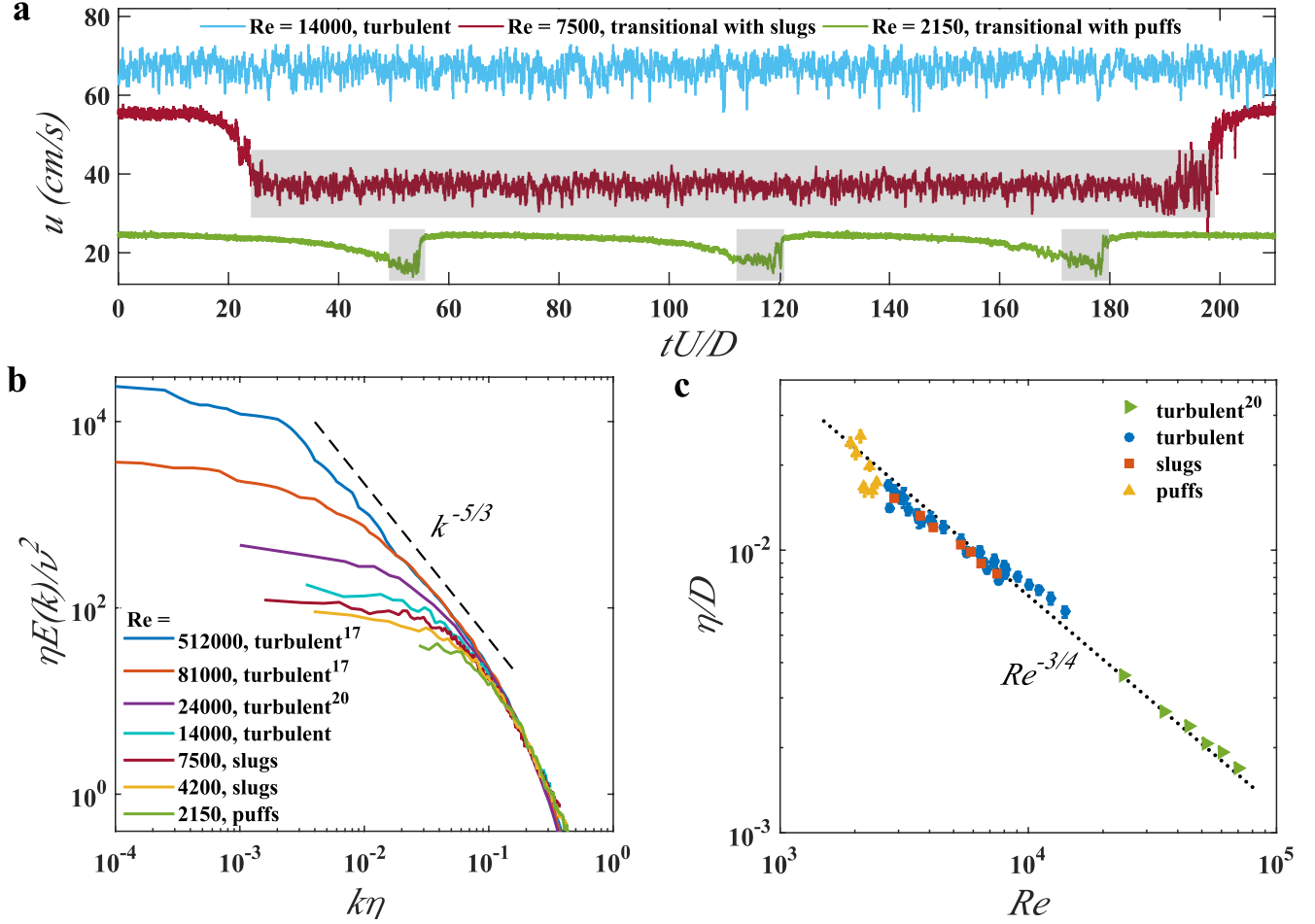


FIG. 3. Tests of Kolmogorov's phenomenological theory of turbulence, Eqs. (1) and (2), for flash flows. (a) Time series of the axial velocity u at the centerline of the pipe for three representative flows. (For the transitional flow with puffs, we plot $1.5u(t)$ for the sake of clarity.) The segments of $u(t)$ that correspond to slugs and puffs have been shaded in grey. We use those segments to compute the spectra $E(k)$ and the viscous lengthscale η for slug flow and for puff flow. (b) Plots of the rescaled spectra $\eta E(k)/\nu^2$ vs. $k\eta$ for a few representative flows, including turbulent flows and flash flows. The rescaled spectra are in good keeping with small-scale universality (Eq. (1)), irrespective of the type of flow. (c) Data points $(\eta/D, Re)$ for all our experiments and for a few high- Re Princeton superpipe experiments [20], showing agreement with the Kolmogorovian scaling of Eq. (2).